

Preparation of Activated Carbon Derived From Licorice Residue and its Electrochemical Properties

Kaiqiang Yi, Yves Iradukunda, Fenfang Luo, Yawen Hu, Xin Li, Guoying Wang, Gaofeng Shi*

School of Petrochemical Engineering, Lanzhou University of Technology, Lan gong ping Road, Lanzhou, Gansu, China

*E-mail: 1172973233@qq.com

Received: 19 October 2020 / Accepted: 8 December 2020 / Published: 31 January 2021

Licorice residue was used as the raw material and pre-carbonized to form a preliminary carbon skeleton at 400 °C followed by activation with KOH and carbonization at 800 °C for 2 hours to produce bio-carbon. Nevertheless, the specific surface area of the prepared carbon was 2103 m²/g which shows KOH has strong pore expansion performance. So far, GC-C03 obtained has a specific capacitance of 320 F/g at 0.5 A/g in a 6 M KOH aqueous solution, very good cycle stability under 1 A/g after 5000 charging and discharging cycles, and can retain 93%. However, to encourage the production of biomass energy, the potential development of supercapacitor and electrode materials presents new ideas for reusing licorice residue which is crucial for green energy production.

Keywords: Licorice residue; Carbonization; pores expansion; electrochemical performance

1. INTRODUCTION

In recent years, with rapid economic development, fossil energy has faced important problems such as resource shortage and serious environmental pollution[1]. As people's requirements for the environment continue to increase, new energy sources such as wind energy and hydropower are developing rapidly, and energy storage materials for new energy sources have become more and more popular. Supercapacitor energy storage device not only has good energy storage performance, it is convenient, efficient, and cheap, but also does not harms the environment [2,3]. As a green energy storage device, it has been used in military and civilian fields such as automobiles and aerospace [4–7]. There are three major types of supercapacitors: double-layer electrical capacitors, pseudo-faraday capacitors, and hybrid capacitors. Electrode material efficiency is the secret to supercapacitors. The benefits of porous carbon materials are commonly used, such as large specific surface area, high conductivity, stable cycle, stable structure, and low price. The preparation of electrode materials from

porous carbon biomass has become a hot spot in particular [8–10]. Licorice residue, which has great output value in Northwest China, is the raw material used in this experimental research. The remains of licorice collected during the extraction of the active ingredient produce a substantial volume of licorice waste, which is deemed to be useless in the fields of dead grass and pollutes the environment. Further production of the residue of licorice and the preparation of electrode materials also significantly increases its economic benefits. The methods of pre-expansion and secondary KOH expansion in this experiment make the prepared carbon have good electrochemical performance and high specific surface area, thereby improving the efficiency of its electricity storage.

2. EXPERIMENTAL

2.1. Reagents

Potassium hydroxide, hydrochloric acid, acetylene black, absolute ethanol, polytetrafluoroethylene

2.2. Equipment

Crusher, tube furnace, vacuum drying oven, electronic balance, sand core funnel, electrochemical workstation

2.3. Pre-carbonization and activation

After extraction, the licorice residue was crushed into powder and filtered with a 100 meshes sieve. The sieved materials were washed several times with ethanol and distilled water to remove impurities and then dried in an oven for 12 h. 20g of pretreated licorice powder was heated at 400°C for 2h at a rate of 5°C/min in a tube furnace in a nitrogen environment and then the temperature was decreased at a rate of 5°C/min. Afterward, the carbon was washed with distilled water and dried in the oven for subsequent use.

Besides, 2 g of pre-carbonized carbon was weighed and mixed with 20% KOH solution at different mass ratios (1:0; 1:0.5; 1:1; 1:1.5) , and then treated with ultrasonic at 50 °C for 30 minutes. After that dried in a vacuum oven for 24h at 80 °C. The prepared samples were labeled as GC-C01, GC-C02, GC-C03, GC-C04 corresponding to the mass ratio of 1:0; 1:0.5; 1:1; 1:1.5.

2.4. Carbonization

In a tube furnace under a nitrogen atmosphere, the pre-carbon was carbonized for 2 h at 800 °C with an increasing and decreasing rate of 5°C/min. The obtained porous carbon was soaked with 2 M

hydrochloric acid solution for 24h, then washed to the neutral with distilled water, and put in a vacuum drying oven at 80 °C for 24h.

2.5. Structure characterization

The surface structure of the porous carbon was observed by cold field emission type scanning electron microscopes (SEM, JSM-6701F Japan Electron Optics) and transmission electron microscopy (TEM, TECNAL G2 TF20USA FEI Co., Ltd.). The pore size distribution and specific surface area of the samples were tested by adsorption and desorption of nitrogen gas in a Micromeritics ASAP 2420 surface analyzer. To assess the crystal structure of the sample, the MSA-XD2 powder X-ray diffractometer (diffraction angle scanning range is 5 to 80°C) was used. A spectrometer (JYHR800, Micro-Raman) measured the Raman spectrum. X-ray photoelectron spectroscopy (XPS, PHI5702, USA) was used to test the surface structure.

2.6. Electrochemical characterization

The mass ratio of porous carbon, acetylene black, and polytetrafluoroethylene were 0.8, 0.15, 0.05, respectively. Then thoroughly mixed and coated with 1×2 cm foam nickel to cover the region of 1×1 cm, put it in a drying oven and dried for 24 hours[11]. It was then pressed at a pressure of 10 MPa for 1 min using the tablet unit. And the three-electrode device with 6 M KOH as the electrolyte, in the voltage range of -1.0-0V, sequentially conduct the test of cyclic voltammetry (CV), galvanostatic current charge and discharge (GCD), impedance (EIS) and cycle life, the basic capacitance of the material was calculated according to the following formula[12].

$$C_s = \frac{I\Delta t}{m\Delta V}$$

C_s is the specific capacitance (F/g), I is the discharge current (A), Δt is the discharge time (s), m is the mass of the active material (g), and ΔV is the potential window (V).

3. RESULTS AND DISCUSSION

3.1. SEM and TEM

It can be seen from Figure. 1a that the untreated carbon materials have almost no pores, it can be shown from Figure.1(b-c) that the substance has large pores and an apparent carbon skeleton. This is because, before the expansion of potassium hydroxide, the process of pre-carbonization has already formed a carbon skeleton, stopping the expansion of potassium hydroxide's very powerful process of which caused the aperture to break. It can be seen from Figure.1d that micropores exist, and it can be seen from Figure.1(e-f) that mesopores exist, so there are micropores, mesopores, and macropores in GC-C03. It is a porous graded carbon, which improves its electrochemical performance.

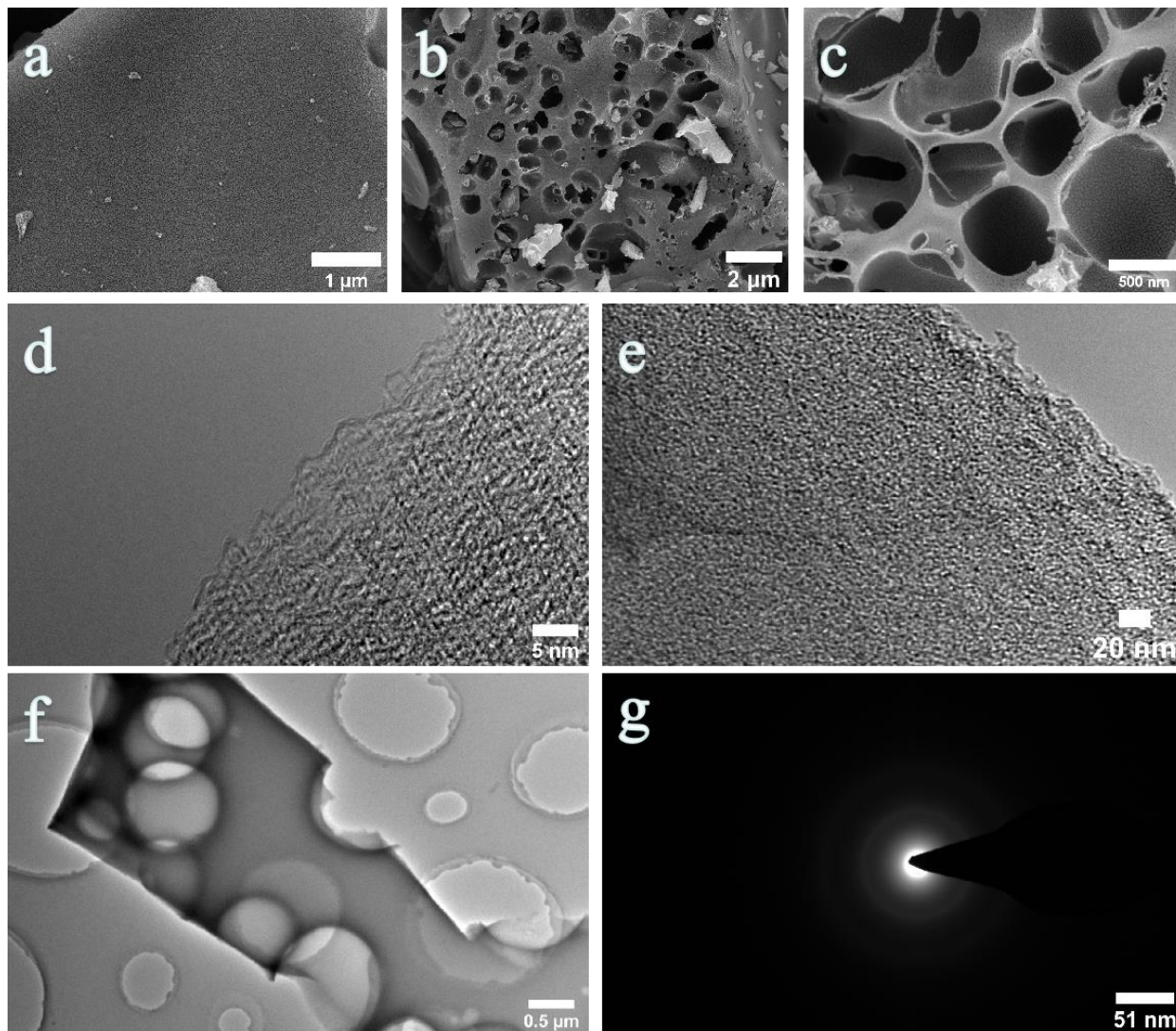


Figure 1. (a) SEM image of GC-C01; (b-c) SEM images of GC-C03; (d-f) TEM images of GC-C03; (g) the selected area diffraction pattern

3.2. XPS spectrum

Figure 2 shows the X-ray electron energy spectrum of GC-C03. Figure.2a is the full spectrum of the sample. There are two main elements of the sample, are C and O. The content of the C element is 93.0%, and the content of the O element is 6.6%. Figure.2b is the C spectra of GC-C03, it can be seen that there are C=C bond (284.6eV), C-O bond (285.5eV), C=O bond (286.5eV), and COOH (289.3eV)[13]. And the main C element of this material is mainly C=C bond, and a small amount of C=O bond, O=C=O bond. Figure.2c is the XPS spectrum of O element, which can be seen that the O element of this material are mainly C=O bond (532.7eV), C-O bond (531.6eV), and O=C-O bond (533.7eV) [14].

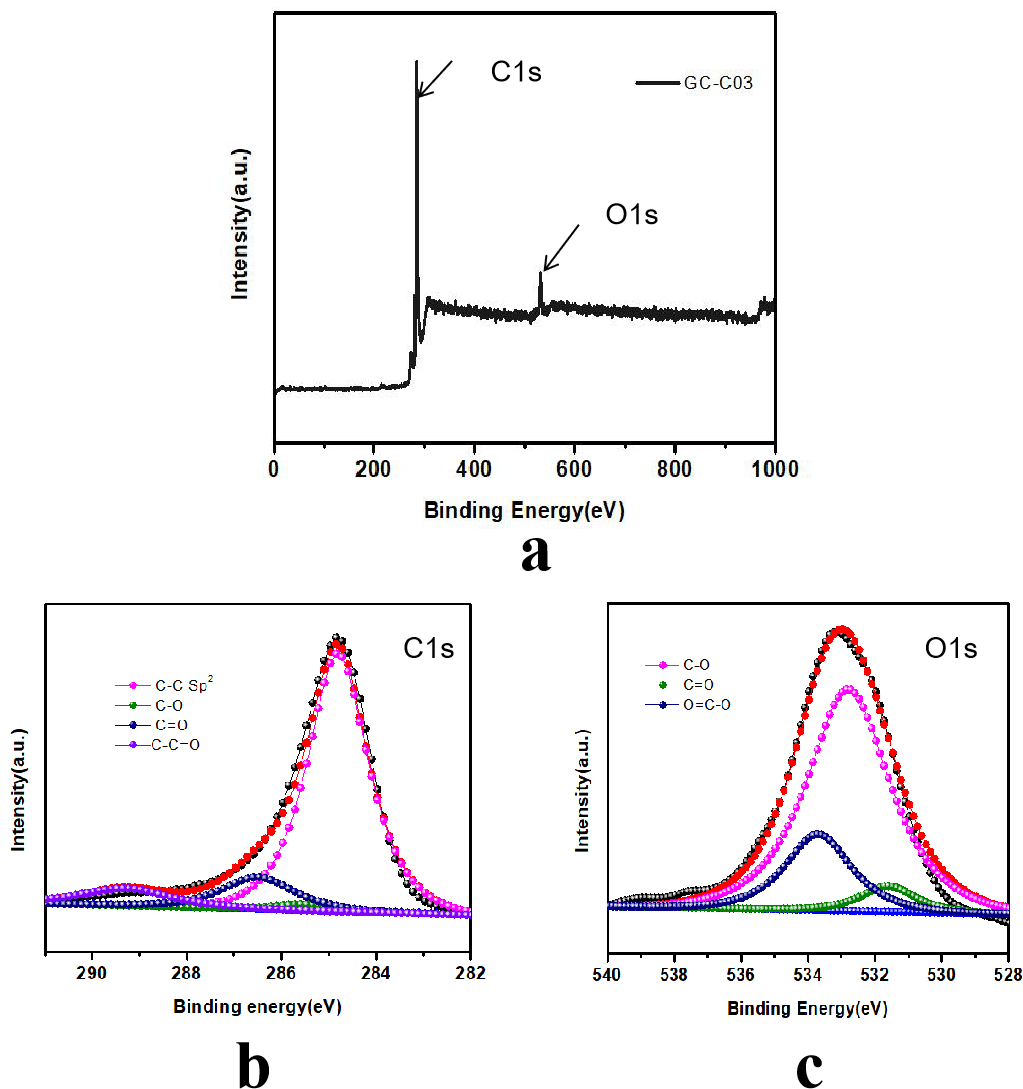


Figure 2. (a)XPS survey spectra of GC-C03, (b-c); C1s and O1s spectra of the GC-C03sample.

3.3. XRD and Raman spectra

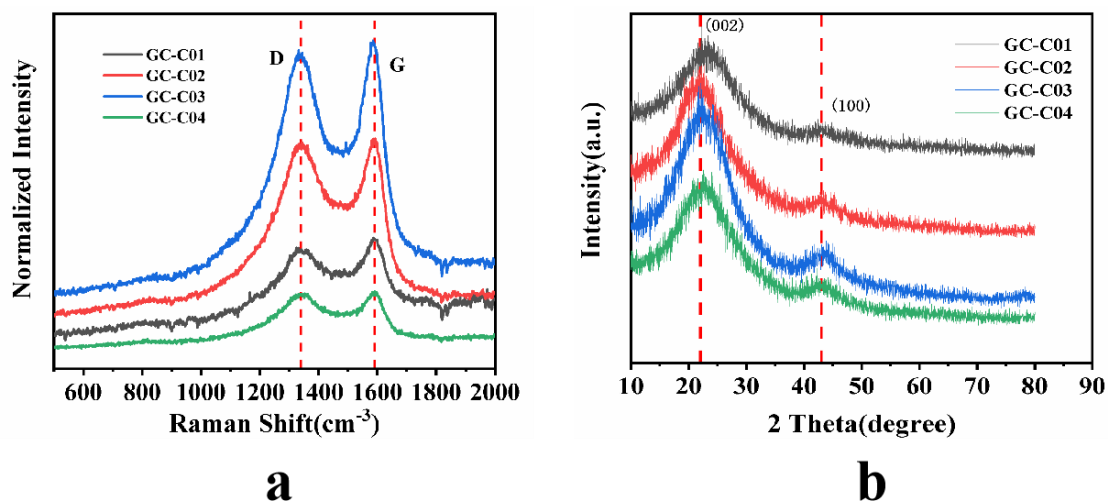


Figure 3. (a) Raman spectra of four samples; (b) XRD patterns of four samples

The samples were analyzed by XRD to determine the crystal structure. The prepared carbon materials have two apparent characteristic peaks at 22.5° and 43.5° , corresponding to the graphite and layer (002) crystal plane and the amorphous carbon (100) crystal planes, as shown in Figure.3a. Furthermore, no other peaks emerged, suggesting that there were few impurities and high purity in the prepared carbon[15,16]. The spectroscopic Raman characterization of the four materials is shown in Figure.3b two characteristic peaks, named the D peak at 1340cm^{-1} and the G peak at 1590cm^{-1} can be observed. Peak D reflects atomic lattice defects, peak G reflects C atom sp^2 hybridization's in-plane stretching vibration. The degree of structural disorder and graphitization of carbon materials can be reflected by I_D / I_G [17,18]. The values of I_D / I_G of GC-C01, GC-C02, GC-C03, and GC-C04 are 0.91, 0.93, 0.95, 0.98, respectively, and it can be concluded that the carbon content has a high degree of disorder after activation of KOH. This is due to the destruction of the carbon layer structure of the carbon material during the activation phase of KOH, making it a more porous structure, Consistent with the conclusion of the SEM image.

3.4. BET analysis

The porous characteristics of the carbon materials of the prepared biomass have been studied. The adsorption-desorption isotherm of porous carbon in nitrogen is shown in Figure.4a and is shown as a typical IV type of adsorption/desorption isotherm, which suggests that there coexist microporous and mesopore [19–21]. At lower relative pressure, the adsorption volume of the sample GC-C03 fell dramatically, suggesting the presence of a large number of micropores; at a higher relative pressure, a retention ring appeared for adsorption of nitrogen, thus indicating the existence of mesopores. The study was consistent with the SEM image characterization. Figure.4b demonstrates the pore size distributions of the four samples. It can be seen that the average pore diameter of the GC-C03 is 1.97nm, thus the material is the kind of micropores materials. it is consistent with the SEM and TEM results that is the activation of KOH makes it a greater specific surface area[22].

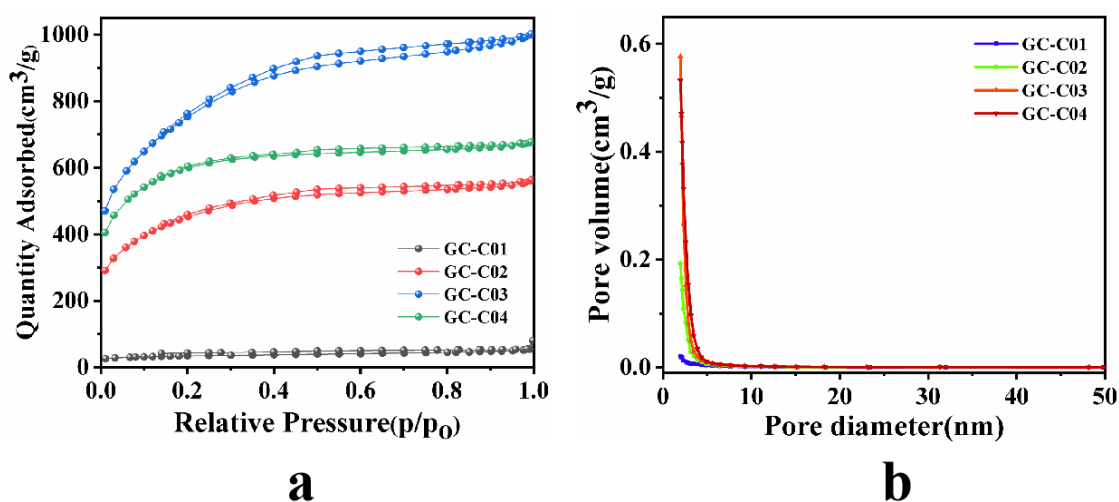


Figure 4. The nitrogen adsorption/desorption isotherm of the sample and Sample method for BJH calculation of pore size distribution.

Table 1. The pore size distribution of porous carbon

Samples	S_t (m^2g^{-1})	V_t (cm^3g^{-1})	V_{micro} (cm^3g^{-1})	V_{meso} (cm^3g^{-1})
GC-C01	117.78	0.08	0.03	0.05
GC-C02	991.95	0.51	0.25	0.26
GC-C03	2103.45	1.04	0.44	0.60
GC-C04	1616.22	0.85	0.19	0.66

S_t : total surface area; V_t : total pore volume; V_{micro} : microspore volume; V_{meso} : mesopore volume

The table reveals that GC-C01, GC-C02, GC-C03, and GC-C04 have unique surface areas of $117.78 m^2g^{-1}$, $991.95 m^2g^{-1}$, $2103.45 m^2g^{-1}$, and $1616.32 m^2g^{-1}$, respectively. The four materials have the highest amount of mesoporous pore, which means that they are predominantly mesoporous. With a total pore volume of $1.04 cm^3g^{-1}$ and a mesopore volume of $0.60 cm^3g^{-1}$, accounting for 57.7% of the total pore volume, the GC-C03 has the most defined pore structure, means that the structure of porous carbon is essentially mesoporous.

3.5. Electrochemical performance

The sample output was calculated with three electrodes system using a 6 M KOH aqueous solution. Figure.5a displays the GCD of four carbon materials under 1 A/g current density and the basic capacitances of GC-CO1, GC-CO2, GC-CO3, and GC-CO4 are 98, 238, 291, and 230 F/g, respectively. GC-CO3 can be shown to have the largest specific capacitance, Figure.5b display CV curves of all samples at a scanning rate of 10mV/s, they all have an internal rectangular form, suggesting that they have common characteristics of electrical double-layer capacitance. The largest area of GC-CO3 depicts that it is the most excellent material among all the samples. Figure.5c demonstrates the impedance curves (EIS) of four carbon products[23–25]. The GC-CO2, GC-CO3, GC-CO4 radius is small in the high-frequency area and the low-frequency region is almost vertical while GC-CO1 has a large radius in the high-frequency region and a small radius in the low-frequency region. This suggests that the other three carbon products have small internal resistance and charge transfer resistance compare to GC-CO1. The GC-CO3 has the best results in capacitance reliability. The CV curve scanning of GC-CO3 with a scanning rate varying from 5 to 100 mV/s as shown in Figure.5d. At various scanning rates, it can stably retain a rectangular-like shape and GCD curve of GC-CO3 at a current density of 0.5 to 20 A/g as shown in Figure.5e. Indeed, from 0.5A/g to 10A/g, the basic capacitance exceeds 322F/g. This shows that the capacitance can still retain 235F/g, and the capacitance retention rate is 73% of GC-CO3 and after 5000 cycles of charging and discharging at 1A/g current density, cycle performance sustains 93% as shown in Figure.5f.

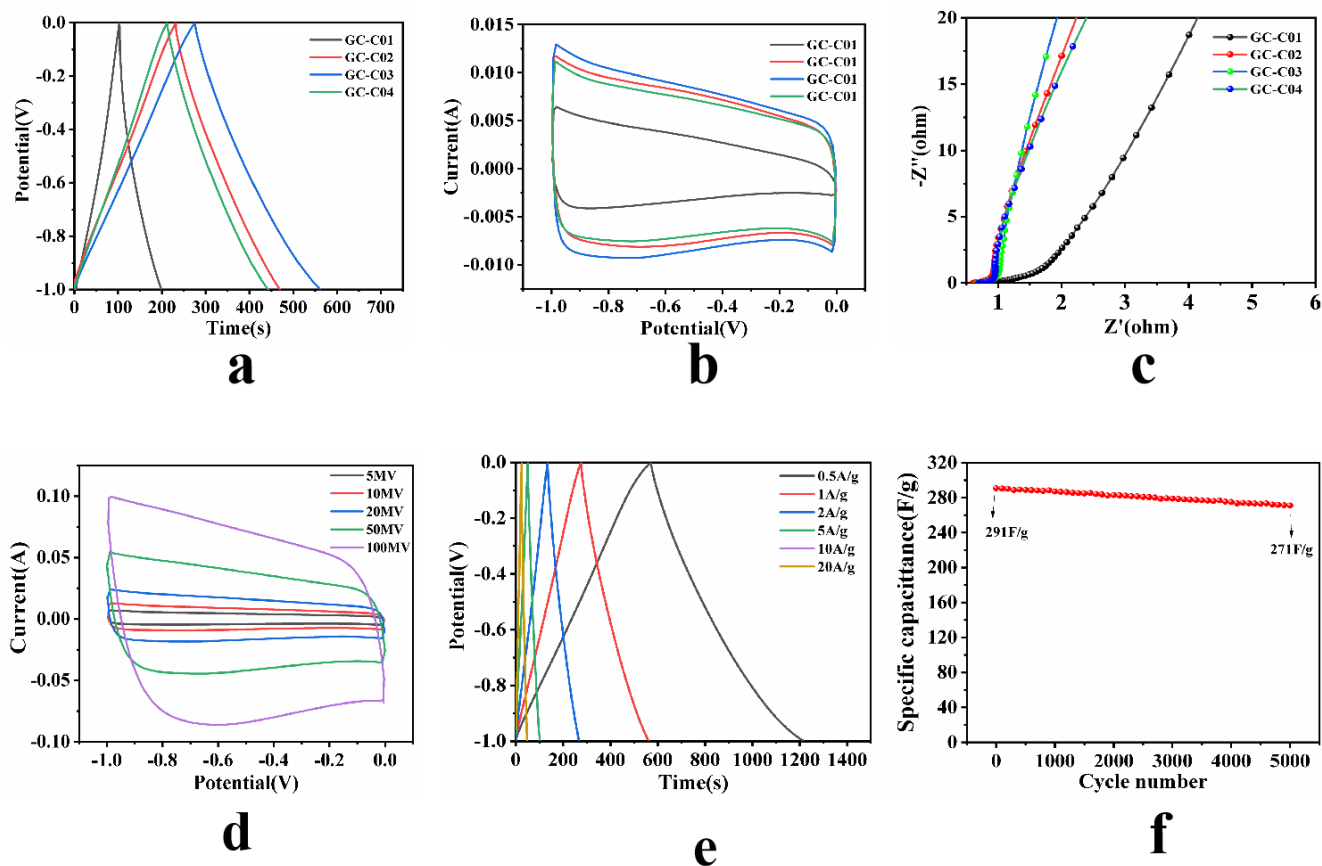


Figure 5. Electrochemical performance of the samples measured in a three-electrode system. (a)GCD curves of all the samples at the current density of 1A/g; (b)CV curves of all the samples at a scan rate of 10mV/s; (c)EIS of all the samples; (d)CV curves for GC-C03 at scan rates ranging from 5mV/s to 100mV/s;(e) GCD curves of GC-C03 at different current densities; (f)GC-C03 in specific capacitance retention rates at the current density of 1A/g after 5000 cycles.

Table 2. The specific capacitance of carbon materials with different activator ratios

Sample	GC-C01	GC-C02	GC-C03	GC-C04
Specific capacitance (F·g ⁻¹)	98	238	291	230

Table 3. Comparison of electrochemical performance of porous carbon with other different materials

Biomass precursor	Electrolyte	Specific capacity(F/g) (current density)	SBET (m ² g ⁻¹)	Reference
Fujimoto bean	6M KOH	219(1 A /g)	1159	[10]
Camellia pollen	2M KOH	205(0.5 A /g)	526	[13]
Industrial hemp straw	6M KOH	244(1 A /g)	2348	[22]
rice straw	1M Na ₂ SO ₄	400(0.1 A /g)	3333	[23]
silkworm excrement	6M KOH	401(0.5 A /g)	2258	[24]
Licorice	6M KOH	320(0.5 A /g)	2103	This work

4. CONCLUSION

In summary, licorice residue was used as a source of carbon in this experiment, and porous carbon was primed by pre-carbonization and supplemented by carbonization, then using KOH as an activator to expand the pores. GC-C03's surface area was 2103 m²/g and a total pore volume of 1.04 cm³/g which showed high pore expansion efficiency for KOH. Indeed, at a current density of 0.5 A / g, the specific capacitance is 320 F/g, and the capacitance retention rate reaches 73 % as the current density increases from 0.5 A/g to 10 A/g. Hence, the results suggest that porous carbon is not only an outstanding supercapacitor electrode substrate but also a good carrier for energy production resulted from licorice residues.

NOTES

The authors declare no conflicts of interest.

ACKNOWLEDGMENTS

This work was supported by the National Key R & D Program of China (No. 2016YFC0202900), the National Natural Science Foundation of China (No. 21567015, 21407072), the Natural Science Foundation of Gansu Province (No. 18JR3RA079, 17JR5RA109), the Project of Food and Drug Administration of Gansu Province (No. 2018GSFDA014), the Gansu Provincial Party Committee Young Creative Talents (No. Ganzutongzi[2017]121), the Hongliu Science Fund for Distinguished Young Scholars (2018), and Lanzhou University of technology Hongliu first-class discipline construction program.

References

1. G. Wang, Y. Iradukunda, G. Shi, P. Sanga, X. Niu and Z. Wu, *J. Environ. Sci.*, 99 (2021) 324.
2. A.G. Pandolfo and A.F. Hollenkamp, *J. Power Sources*, 157 (2006) 11.
3. M. Jung, E. Jeong, Y. Kim, and Y. Lee, *J. Ind. Eng. Chem.*, 19 (2013) 1315.
4. V.A. Online, E. V Kondratenko and G. Mul, J. Baltrusaitis, *Energy Environ. Sci.*, 6 (2013) 3112.
5. D.G. Nocera, *Chem. Soc. Rev.*, 38 (2009) 13.
6. S. Chu and A. Majumdar, *Nature*, 488 (2012) 1.
7. A.C. Dillon, *Chem. Rev.*, 110 (2010) 6856.
8. C. Ma, J. Shi, Y. Li, Y. Song, and L. Liu, *Carbon N. Y.*, 95 (2015) 1082.
9. D. Jin, X. Yang, M. Zhang, B. Hong, H. Jin, X. Peng, J. Li, H. Ge, X. Wang, Z. Wang and H. Lou, *Mater. Lett.*, 139 (2015) 262.
10. G. Shi, Z. Wang, C. Liu, G. Wang, S. Jia, X. Jiang, Y. Dong, and Q. Zhang, *Int. J. Electrochem. Sci.*, 14 (2019) 5259–5270.
11. X. Zhao, P. Li, S. Yang, Q. Zhang, and H. Luo, *Ionics (Kiel)*, 23 (2017) 1.
12. M. Yu, T. Zhai, X. Lu, X. Chen, S. Xie, W. Li, C. Liang, W. Zhao, L. Zhang, and Y. Tong, *J. Power Sources*, 239 (2013) 64.
13. C. Lu, J. Li, and J.P. Cheng, *J. Power Sources*, 394 (2018) 9.
14. H. Chen, Y. Guo, F. Wang, G. Wang, P. Qi, X.H. Guo, B. Dai, and F. Yu, *New Carbon Mater.*, 32 (2017) 592.
15. C. Ma, R. Wang, Z. Xie, H. Zhang, Z. Li, J. Shi, *J. Porous Mater.*, 24 (2017) 1437.
16. D. Zhang, M. Han, Y. Li, J. He, B. Wang, K. Wang, and H. Feng, *J. Power Sources*, 372 (2017) 260.
17. K. Kakiage, Y. Aoyama, T. Yano, K. Oya, J. Fujisawa and M. Hanaya, *R. Soc. Chem.*, 00 (2013) 1.

18. L. Zhang, Y. Jiang, L. Wang, C. Zhang, and S. Liu, *Electrochim. Acta*, 196 (2016) 189.
19. Y. Ou, C. Peng, J. Lang, D. Zhu and X. Yan, *Carbon N. Y.*, 29 (2014) 193.
20. H. Lu, W. Dai, M. Zheng, N. Li, G. Ji, and J. Cao, *J. Power Sources*, 209 (2012) 243.
21. J. Rantanen, *J. Pharm. Pharmacol.*, 59 (2007) 171.
22. G. Shi, C. Liu, G. Wang, X. Chen, L. Li, X. Jiang, P. Zhang, Y. Dong, S. Jia, H. Tian, Y. Liu, Z. Wang, Q. Zhang and H. Zhang, *Ionics (Kiel)*, 25 (2019) 1805.
23. H. Jin, J. Hu, S. Wu, X. Wang, H. Zhang, and H. Xu, *J. Power Sources*, 384 (2018) 270.
24. S. Lei, L. Chen, W. Zhou, P. Deng, Y. Liu, L. Fei, and W. Lu, *J. Power Sources*, 379 (2018) 74.
25. W. Li, F. Zhang, Y. Dou, Z. Wu, H. Liu, X. Qian, D. Gu, Y. Xia, B. Tu, and D. Zhao, *Adv. Energy Mater.*, 7 (2011) 382.

© 2021 The Authors. Published by ESG (www.electrochemsci.org). This article is an open access article distributed under the terms and conditions of the Creative Commons Attribution license (<http://creativecommons.org/licenses/by/4.0/>).